

Fault Detection of DC Electric Motors Using the Bispectral Analysis

MIHA BOLTEŽAR* and JANKO SLAVIČ

University of Ljubljana, Faculty of Mechanical Engineering, Aškerčeva 6, 1000 Ljubljana, Slovenia

(Accepted: 9 September 2005)

Abstract. The two major advantages of bispectral analysis are: resistance to noise and the ability to detect nonlinearities, like quadratic phase coupling. The first aim was to study some of the theoretical aspects of bispectral estimation. A lot of attention was paid to the influence of noise, the number of segments, the influence of one or several harmonic deterministic components and aliasing. These aspects are typical of rotating machinery. An example of successful fault identification in DC electric motors is presented. The identification proved to be capable to identify quadratically coupled mechanical system when the power-spectra analysis failed. Further it proved to be quite resistant to noise.

Key words: Bispectral analysis, Bicoherence, DC electric motor, Fault detection, Condition monitoring.

1. Introduction

The second-order spectral analyses provide basic information about a process. However, higher-order spectral (also known as polyspectra) analyses are able to provide some new characteristics of the analyzed process. In contrast to second-order spectra (e.g. power spectra), which are obtained relatively easily and can be interpreted in a straightforward manner, higher-order spectra demand a great deal of effort and the interpretation of the results is not so clear. In nonlinear systems, however, the second-order spectra are insufficient, and therefore in this study the bispectra will be used for the identification of quadratic phase-coupled (QPC) systems [1].

The major advantages of bispectra are as follows: *the identification of nonGaussian processes, the filtering out of Gaussian noise* [2], *the identification of certain types of nonlinearity* [3], *and the testing for aliasing* [4].

In mechanical engineering the bispectral analysis has mostly been applied to the condition monitoring of different machinery. Examples of this type of monitoring include: stamping operations [5], the diagnosis of the condition of motor bearings [6], fault identification in rotating machinery [7], condition monitoring in reciprocating machines [8], wind turbine blades [9], cutting-process identification [10] and diagnosis of planar dynamics of nonlinear systems [11, 12].

In bispectral analyses the spectral leakage and therefore the choice of window is very important. The reader is referred to Fackrell's excellent review of the various windows [3]. Since the calculation of the bispectrum can be time consuming, and

*Author for correspondence: e-mail: miha.boltezar@fs.uni-lj.si

because of the statistical properties of bispectra, special attention needs to be paid to the proper re-sampling of the signal [13–15].

The second section covers some of the basics of higher-order spectral analysis. The third section presents some of the important properties for the identification of QPC signals, while the actual identification of the QPC signals is given in the fourth section. In the following two sections a numerical and a real experiment are analyzed. The last section is devoted to conclusions.

2. The Basics of Higher-order Spectral Analysis

2.1. THE APPLICATION OF MOMENTS

For a set of n , real, random, continuous and stationary processes $\{x_1, x_2, \dots, x_n\}$ the r^{th} ($r = k_1 + k_2 + \dots + k_n$) order joint moment is defined by [16]:

$$\begin{aligned} m_r &= \text{Mom}[x_1^{k_1}, x_2^{k_2}, \dots, x_n^{k_n}] \triangleq E[x_1^{k_1} x_2^{k_2} \dots x_n^{k_n}] \\ &= (-i)^r \frac{\partial^r \Phi(\omega_1, \omega_2, \dots, \omega_n)}{\partial \omega_1^{k_1} \partial \omega_2^{k_2} \dots \partial \omega_n^{k_n}} \Bigg|_{\omega_1=\omega_2=\dots=\omega_n=0}, \end{aligned} \quad (1)$$

where $E[\cdot]$ is the expectation operator, $i = \sqrt{-1}$ and $\Phi(\cdot)$ is the (first) joint characteristic function, also called the moment generation function (MGF) [3]:

$$\Phi(\omega_1, \omega_2, \dots, \omega_n) = E[e^{i(\omega_1 x_1 + \omega_2 x_2 + \dots + \omega_n x_n)}]. \quad (2)$$

From (1) it follows that the first coefficient of the Taylor expansion of the MGF function is the mean value (3), the second is its variance (4), ...

$$m_1 = E[x_1] \quad (3)$$

$$m_2 = E[x_1^2] \quad (4)$$

⋮

2.2. THE APPLICATION OF CUMULANTS

Similarly to the role of the first joint characteristic function Φ for moments is the role of the second joint characteristic function (also called the cumulant generation function – CGF), for the cumulants:

$$\Psi(\omega_1, \omega_2, \dots, \omega_n) \triangleq \ln(\Phi(\omega_1, \omega_2, \dots, \omega_n)). \quad (5)$$

The Taylor expansion of the second characteristic function defines the joint cumulants:

$$\begin{aligned} c_r &= \text{Cum}[x_1^{k_1}, x_2^{k_2}, \dots, x_n^{k_n}] \\ &\triangleq (-i)^r \frac{\partial^r \Psi(\omega_1, \omega_2, \dots, \omega_n)}{\partial \omega_1^{k_1} \partial \omega_2^{k_2} \dots \partial \omega_n^{k_n}} \Bigg|_{\omega_1=\omega_2=\dots=\omega_n=0}. \end{aligned} \quad (6)$$

If $r = n$, then the cumulants are related to the moments [16]:

$$c_1 = \text{Cum}[x_1] = m_1 \tag{7}$$

$$c_2 = \text{Cum}[x_1, x_1] = m_2 - m_1^2 \tag{8}$$

$$c_3 = \text{Cum}[x_1, x_1, x_1] = m_3 - 3m_2 m_1 + 2m_1^3 \tag{9}$$

$$c_4 = \text{Cum}[x_1, x_1, x_1, x_1] \\ = m_4 - 4m_3 m_1 - 3m_2^2 + 12m_2 m_1^2 - 6m_1^4. \tag{10}$$

For a given, real random process $\{X(k)\}$, where $k = 0, \pm 1, \pm 2, \dots$ the moments up to order n are defined by:

$$\text{Mom}[X(k), X(k + \tau_1), \dots, X(k + \tau_{n-1})] \\ = E[X(k) X(k + \tau_1) \cdots X(k + \tau_{n-1})]. \tag{11}$$

If the first-order moment (average) is equal to zero, i.e. $m_1 = 0$, then the second- and third-order cumulants are defined as:

$$c_2(\tau_1) = m_2(\tau_1) \tag{12}$$

$$c_3(\tau_1, \tau_2) = m_3(\tau_1, \tau_2). \tag{13}$$

The second-order cumulant is used for the calculation of the power spectrum:

$$C_2^x(\omega) = \sum_{\tau=-\infty}^{+\infty} c_2^x(\tau) e^{-i\omega\tau}, \tag{14}$$

where:

$$|\omega| \leq 2\pi \frac{f_s}{2}. \tag{15}$$

f_s is the sampling frequency.

The Fourier transform of the third-order cumulant defines the bispectrum:

$$C_3^x(\omega_1, \omega_2) = \sum_{\tau_1=-\infty}^{+\infty} \sum_{\tau_2=-\infty}^{+\infty} c_3^x(\tau_1, \tau_2) e^{-i(\omega_1 \tau_1 + \omega_2 \tau_2)}, \tag{16}$$

where:

$$|\omega_1| \leq \pi f_s \quad \& \quad |\omega_2| \leq \pi f_s \quad \& \quad |\omega_1 + \omega_2| \leq \pi f_s \tag{17}$$

The frequency pair (ω_1, ω_2) is called the bifrequency.

Equation (16) represents the indirect method. On the other hand, the direct method of the bispectrum is calculated in the frequency domain [2]:

$$B(\omega_1, \omega_2) = \mathcal{X}(\omega_1) \mathcal{X}(\omega_2) \mathcal{X}^*(\omega_1 + \omega_2), \tag{18}$$

where $\mathcal{X} = \mathcal{F}(X)$ (the Fourier transform) and \mathcal{X}^* denotes the complex conjugate of \mathcal{X} .

In general, there are two ways to estimate the bispectrum: by segments averaging and by frequency averaging [17]. In this study only the first of these will be presented.

For a real signal X of length N we therefore create K segments, each of length M . To achieve a better frequency resolution on short signals the segments can overlap. However, to keep the inter-segment correlation low more than 50% of overlapping is not advised. The segments-averaged bispectrum estimate is defined as:

$$\hat{B}(\omega_1, \omega_2) = \frac{1}{K} \sum_{i=1}^K \hat{B}_i(\omega_1, \omega_2). \quad (19)$$

Hinich [2] demonstrated that for a real signal X that includes noise the bispectrum estimate \hat{B} is asymptotically unbiased, and that the variance is proportional to the power spectra, as noted:

$$\text{Var } \hat{B}(\omega_1, \omega_2) \propto M C_2(\omega_1) C_2(\omega_2) C_2(\omega_1 + \omega_2). \quad (20)$$

If the segment is longer, then the frequency resolution of the Fourier transform is better. The variance, however, rises (20). Therefore, a balance between the number of segments and the length of the segment is needed. Often these numbers are equal [15]: $K = M$.

Next, from equation (20) it follows that if the power spectra of the signal X is high at frequencies ω_1 , ω_2 and $\omega_1 + \omega_2$, the variance will also be high. As later we will be interested in such signals, this poses a problem that can be reduced in several ways: one way is to add noise to the signal before calculating the bispectrum; the other, which is more often used and also more convenient, is to normalize the bispectrum:

$$\hat{b}(\omega_1, \omega_2) = \frac{\frac{1}{K} \sum_{i=1}^K \hat{B}_i(\omega_1, \omega_2)}{\sqrt{\frac{1}{K} \sum_{i=1}^K |\hat{\mathcal{X}}_i(\omega_1) \hat{\mathcal{X}}_i(\omega_2)|^2 |\hat{\mathcal{X}}_i(\omega_1 + \omega_2)|^2}}. \quad (21)$$

$\hat{b}(\omega_1, \omega_2)$ is the *complex bicoherence*: $0 \leq |\hat{b}| \leq 1$. Later we will refer to biphas which is the argument of the complex bicoherence: $\angle \hat{b} = \arg \hat{b}$.

There are different definitions and also different notations for the bicoherence. In this study only the complex bicoherence (21) will be used. For an overview of the different notations see [3].

3. Bispectrum and Signal Analysis

In this section we look at what can be obtained from cumulants. Only the most useful properties of the moments and cumulants will be discussed, for a complete overview the reader should refer to [3, 4, 16, 17].

3.1. CUMULANTS OF THE SUM OF INDEPENDENT PROCESSES

In the case of independent real, random and stationary processes $\{x_1, x_2, \dots, x_n\}$ and $\{y_1, y_2, \dots, y_n\}$ the cumulant of the sum equals the sum of the cumulants:

$$\text{Cum}[x_1 + y_1, x_2 + y_2, \dots, x_n + y_n] = \text{Cum}[x_1, \dots, x_n] + \text{Cum}[y_1, \dots, y_n] \quad (22)$$

3.2. CUMULANTS OF A GAUSSIAN PROCESS

The probability distribution function (PDF) $f(x)$ of a Gaussian process is:

$$f_G(x) = \frac{1}{\sqrt{2\pi} \sigma} e^{-\frac{x^2}{2\sigma^2}}. \tag{23}$$

From equations (1) and (2) the first characteristic function is derived as:

$$\Phi_G(\omega) = \int_{-\infty}^{+\infty} e^{i\omega x} f_G(x) dx = e^{-\frac{\sigma^2 \omega^2}{2}}, \tag{24}$$

and the second characteristic function for the Gaussian process is:

$$\Psi_G(\omega) = \ln(\Phi_G) = -\frac{\sigma^2 \omega^2}{2}. \tag{25}$$

From the first and the second characteristic function of the Gaussian process and equations (1) and (6) it follows that all the cumulants, except for the cumulant c_2 , are equal to 0. However, this does not hold for the moments. The moments and cumulants of a Gaussian process up to the order 4 are given in Table 1.

It follows that the bispectrum (16) of a Gaussian process is equal to zero at all frequencies. Theoretically, the bispectrum is equal to zero at all frequencies for all processes with a symmetrical probability distribution [3].

3.3. CUMULANTS OF A HARMONIC PROCESS

The probability distribution function of a harmonic process $x(t) = A \cos(\omega t)$ (where t is assumed to be random variable; while it is actually not) is [18]:

$$f_H(x) = \frac{1}{\pi \sqrt{A^2 - x^2}}. \tag{26}$$

The first characteristic function is:

$$\Phi_H(\omega) = \int_{-A}^{+A} e^{i\omega x} f_H(x) dx = J_0(A\omega), \tag{27}$$

where $J_0(A\omega)$ is a Bessel function of the first kind. The second characteristic function is:

Table 1. First four moments and cumulants of Gaussian and harmonic processes

r -order	Gaussian		Harmonic	
	m_r	c_r	m_r	c_r
1	0	0	0	0
2	σ^2	σ^2	$\frac{1}{2}A^2$	$\frac{1}{2}A^2$
3	0	0	0	0
4	$3\sigma^4$	0	$\frac{3}{8}A^4$	$-\frac{3}{8}A^4$

$$\Psi_{\text{H}}(\omega) = \ln(\Phi_{\text{H}}) = \ln(J_0(A\omega)). \quad (28)$$

The moments and cumulants of a harmonic process up to the order 4 are given in Table 1.

Because the harmonic process is deterministic the moments and cumulants are actually phase dependant (τ_1), e.g.: $c_2(\tau_1) = \frac{1}{2}A^2 \cos \dot{\varphi} \tau_1$.

Equation (29) shows that $c_3(\tau_1, \tau_2)$ is equal to zero for every choice of parameters τ_1, τ_2 .

$$\int_{-T/2}^{+T/2} x(t)x(t+\tau_1)x(t+\tau_1) \frac{1}{T} dt = 0, \quad T = \left(\frac{\omega}{2\pi}\right)^{-1}. \quad (29)$$

Because $c_3(\tau_1, \tau_2)$ of a harmonic process is zero it follows that the bispectrum cannot detect it (because is zero). While we are not interested in harmonic but coupled signals we will use this property to our advance.

4. Identification of Quadratic Phase Coupling

At first the quadratic phase coupling (QPC) needs to be defined.

We start with a harmonic signal of the form:

$$y(t) = \cos(\omega_1 t + \varphi_1) + \cos(\omega_2 t + \varphi_2), \quad (30)$$

which passes through a nonlinear filter of the form $(\) + (\)^2$, then on the output a multi-harmonic signal of several amplitudes and frequencies is obtained. These values are given in Table 2. The phase coupling arises from the quadratic nonlinearity, and therefore for such a process the term quadratic phase coupling is used.

While the bispectrum (19) returns a complex number as a multiple of the Fourier transform at frequencies ω_1, ω_2 and $-(\omega_1 + \omega_2)$, the phase (also called the biphas) of the bispectrum of the QPC signal is theoretically zero. See also the arrow-marks in Table 2. From now on the focus will be on the normalized bispectrum estimate: the bicoherence estimate (21).

The identification of the QPC at each bifrequency is made in two steps: first, testing for a significant bicoherence magnitude; and second, testing for a zero biphas.

Table 2. Output of a *nonlinear filter* of the harmonic signal given by equation (30)

	Amplitude	Frequency	Phase	
$\cos(\omega_1 t + \varphi_1)$	1	ω_1	φ_1	\Leftarrow
$+\cos(\omega_2 t + \varphi_2)$	1	ω_2	φ_2	\Leftarrow
$+ 1$	1	0	0	
$+\frac{1}{2} \cos(2\omega_1 t + 2\varphi_1)$	$\frac{1}{2}$	$2\omega_1$	$2\varphi_1$	
$+\cos((\omega_1 + \omega_2)t + (\varphi_1 + \varphi_2))$	1	$\omega_1 + \omega_2$	$\varphi_1 + \varphi_2$	\Leftarrow
$+\cos((\omega_1 - \omega_2)t + (\varphi_1 - \varphi_2))$	1	$\omega_1 - \omega_2$	$\varphi_1 - \varphi_2$	
$+\frac{1}{2} \cos(2\omega_2 t + 2\varphi_2)$	$\frac{1}{2}$	$2\omega_2$	$2\varphi_2$	

For the test of significant bicoherence the following hypotheses are made:

- H_0 : the bicoherence at this bifrequency is zero (there is just Gaussian noise),
- H_1 : the bicoherence at this bifrequency is not zero (there is more than just Gaussian noise).

If the hypothesis H_0 is refused, then there might be a QPC and the procedure continues with the following hypotheses:

- H_0 : the biphas at this bifrequency is zero,
- H_1 : the biphas at this bifrequency is not zero.

If the H_0 is accepted, then a QPC is present.

Haubrich [19] stated that the distribution of a skewness function for a Gaussian process is approximately χ^2 with 2 degrees of freedom. Fackrell [3] showed that from this property for a given significance level α , the highest/critical bicoherence level for accepting the zero hypothesis for bicoherence is:

$$b_{\text{crit}}^2 = -\frac{2\ln(1-\alpha)}{\text{dof}}, \tag{31}$$

where dof is the degree of freedom defined as: $\text{dof} = 2K$, where K is the number of segments.

The distribution of the biphas is approximately normal [14], and the highest/critical biphas for accepting the zero hypothesis for the biphas at the significance level α_p is [3]:

$$\angle b_{\text{crit}} = \frac{\alpha_p}{\sqrt{\text{dof}}} \sqrt{\frac{1}{\hat{b}^2} - 1}, \tag{32}$$

5. Numerical Examples

As the output of the bicoherence is highly dependent on the appropriate set of parameters.

In this numerical example the focus is given to the appropriate number of segments (parameter K) and the segment length (parameter M). Both parameters have to follow some rules.

As real signals allways include noise, there the influence of Gaussian noise added to the signal is studied.

5.1. THE USEFULNESS OF NOISE AND THE IMPORTANCE OF THE NUMBER OF SEGMENTS

A synthetic signal of one QPC component was created, see Figure 1. The synthetic signal was re-sampled to $K = 256$, $M = 256$ (19), and the overlapping was 50%. The

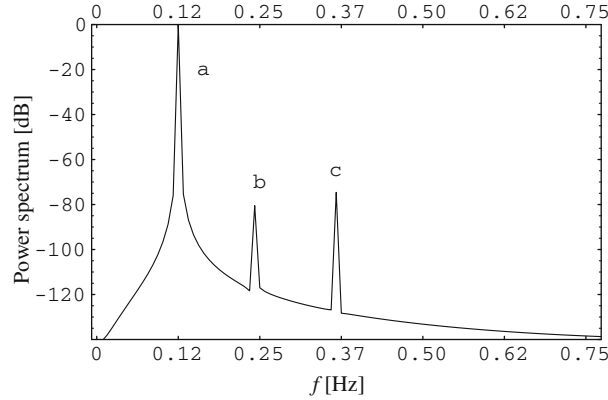


Figure 1. Power spectrum of the synthetic signal (without noise). (a) 0.1249 Hz, (b) 0.2423 Hz, (c) QPC component.

bicoherence squared b^2 and the phase significance were $\alpha = \alpha_p = 0.99$, see equations (31) and (32). The bicoherence estimate of the synthetic signal with added noise of 20 dB (33) is shown in Figure 2. As can be seen the identification of the QPC component is successful. The triangles in the Figure 2 denote the principal domain of the bispectrum; the inter triangle is defined by equation (17) and is of primary interest in this study, for details see i.e. [3].

The noise was described by the signal-to-noise ratio (SNR) in dB:

$$\text{SNR} = 10 \log_{10} \left(\frac{\text{var}(\text{signal})}{\text{var}(\text{noise})} \right). \quad (33)$$

In this study Gaussian noise is used.

However, the identification of QPC on a noiseless signal fails, see Figure 3. When testing synthetic signals for QPC we have to add noise. On real signals this, however, is not usually necessary because the noise is already present. In bispectral analysis noise up to about 20 dB can enhance the identification.

The identification also fails if the number of segments K is small, see Figure 4. It is advisable to use $K = M$ [15].

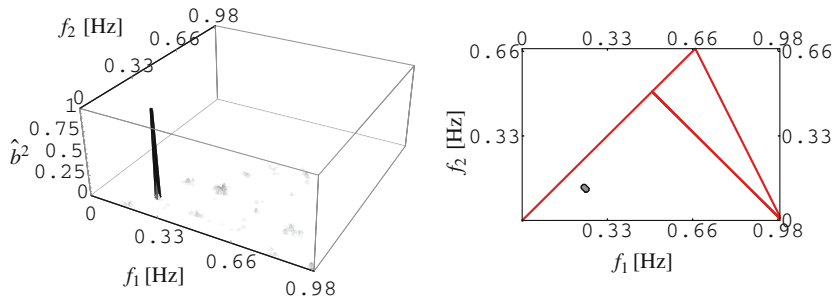


Figure 2. Bicoherence of synthetic signal with SNR = 20 dB.

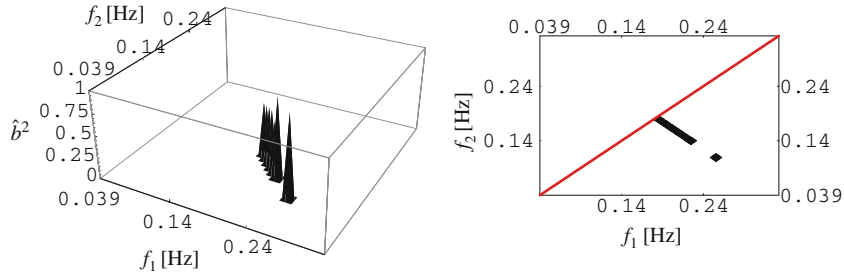


Figure 3. Bicoherence of synthetic signal without noise.

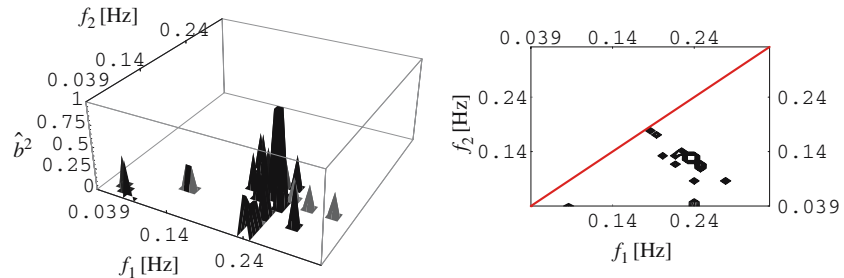


Figure 4. Bicoherence calculated on $K = 16$ segments. SNR = 20 dB.

5.2. HARMONIC SIGNALS

A synthetic signal of 20 harmonic components was created:

$$y(t) = \sum_{i=1}^{20} A_i \cos(2\pi f_i t + \phi_i). \tag{34}$$

Details are given in Table 3, see also Figure 5. From Table 3 it is clear that there are two QPC components: the 3rd and the 6th, where the amplitudes of the latter are very different. Next, the signal also includes a component where only frequencies are coupled and a component where only phases are coupled.

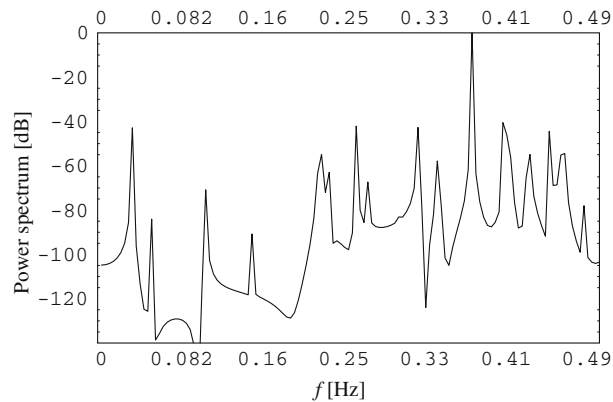


Figure 5. Power spectrum of the synthetic signal.

Table 3. Parameters of the harmonic function

i	A_i	f_i [Hz]	φ_i	i	A_i	f_i [Hz]	φ_i
1	1	0.1050	Random $[0, 2\pi)$	11	1	0.3210	Random $[0, 2\pi)$
2	1	0.1525	Random $[0, 2\pi)$	12	1	0.3751	Random $[0, 2\pi)$
3	1	$f_1 + f_2 = 0.2575$	$\phi_1 + \phi_2$	13	1	0.4320	Random $[0, 2\pi)$
4	0.1	0.3010	Random $[0, 2\pi)$	14	1	0.4670	Random $[0, 2\pi)$
5	1	0.4120	Random $[0, 2\pi)$	15	1	0.0510	Random $[0, 2\pi)$
6	1	$f_2 + f_4 = 0.4535$	$\phi_2 + \phi_4$	16	1	0.3410	Random $[0, 2\pi)$
7	1	$f_1 + f_4 = 0.4060$	Random $[0, 2\pi)$	17	1	0.4880	Random $[0, 2\pi)$
8	1	0.0310	$\phi_1 + \phi_5$	18	1	0.2310	Random $[0, 2\pi)$
9	1	0.2210	Random $[0, 2\pi)$	19	1	0.3710	Random $[0, 2\pi)$
10	1	0.2690	Random $[0, 2\pi)$	20	1	0.4110	Random $[0, 2\pi)$

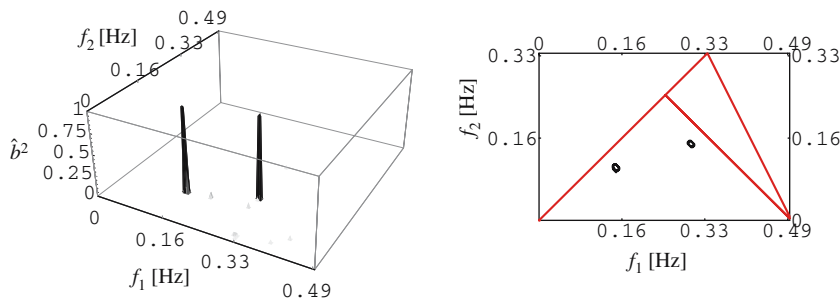
In this study, because of the low leakage, the Hamming window was used. The synthetic signal was re-sampled to $K = 256$, $M = 256$, and the overlapping was 50%. The bicoherence squared b^2 and phase significance were $\alpha = \alpha_p = 0.99$, see equations (31) and (32).

The bicoherence estimate at $\text{SNR} = \infty$ is given in Figure 6. It is clear that there are two peaks that correspond to the QPC components 3 and 6: at the bifrequency (0.1523 Hz, 0.1055 Hz) with value $\hat{b}^2 = 0.9999$ and at the bifrequency (0.3008 Hz, 0.1523 Hz) with the value $\hat{b}^2 = 0.9950$. At the bifrequencies of the only frequency-coupled component, 7, or the only phase-coupled component, 8, as expected, there is no peak.

As the noise increases the identification of the QPC worsens, see Figures 5–9. At about $\text{SNR} = 5$ dB the QPC component 6 disappears. The reason is the very small amplitude of one component of the QPC component 4. At about $\text{SNR} = 0$ dB the QPC component 3 also disappears. While 0 dB means equal variance of noise and signal it can be stated that the QPC identification is very resistant to noise.

5.3. HARMONIC SIGNALS WITH ALIASING

To test the aliasing resistance of the presented methods an additional signal was created: to the previous signal two components were added. Both components had an

Figure 6. Bicoherence of synthetic signal, $\text{SNR} = \infty$ dB.

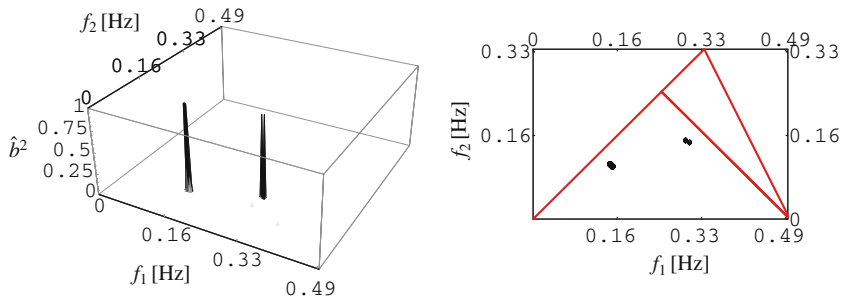


Figure 7. Bicoherence of synthetic signal, SNR = 20 dB.

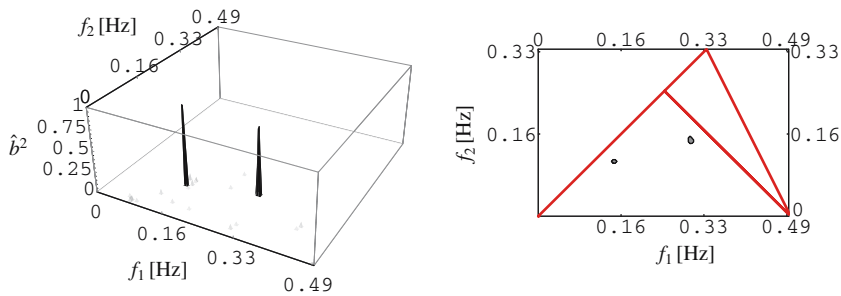


Figure 8. Bicoherence of synthetic signal, SNR = 10 dB.

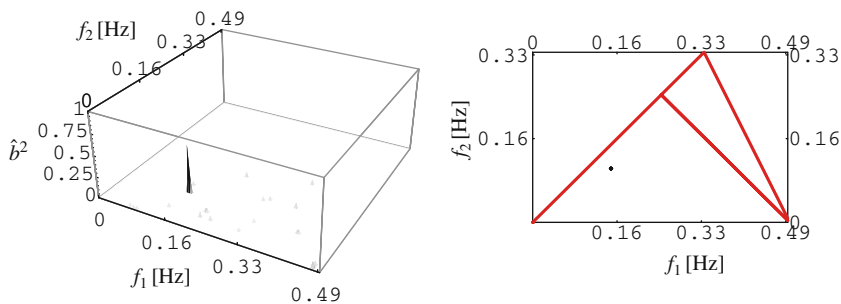


Figure 9. Bicoherence of synthetic signal, SNR = 0 dB.

amplitude $A_{21} = A_{22} = 1$ and random phase, the first with a frequency $f_{21} = 0.5512$ Hz and the second with a frequency $f_{22} = 0.6103$ Hz. Based on the research of Hinich [4], this will affect the identification. In Figure 10 the affect of aliasing is already seen at a SNR = 20 dB. At 10 dB of noise the identification of the QPC components is very low. It is possible to see a small peak at the bifrequency (0.3828 Hz, 0.2226 Hz), and as noted by Hinich, in the case of aliasing the bispectrum of the outer triangle is not zero and this can be used as a hallmark of aliasing.

6. The Detection of Faults in DC Electric Motors Using Bispectral Analyses

In this section we will show how we used the presented knowledge to distinguish a fault in DC electric motor which could not be identified by second order spectral methods.

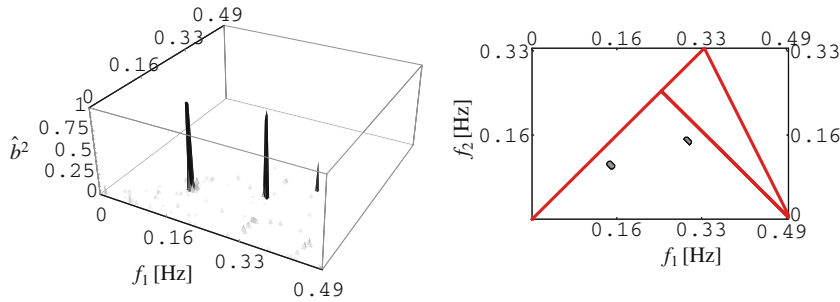


Figure 10. Bicoherence of synthetic signal with aliasing, SNR = 20 dB.

A laser velocimeter was used to provide signals from the vibration at a certain point on a motor housing (Figure 11).

The data were sampled at a frequency of 22 050 Hz, and before calculating the bicoherence estimate it was re-sampled to $K = 256$, $M = 256$ (19), and the overlapping was 50%. The bicoherence and phase significance was $\alpha = \alpha_p = 0.99$, see equations (31) and (32).

Two typical manufacturing faults of DC electric motors will be analyzed: bearing fault and a collector fault.

These mechanical faults have very similar power spectrum (Figures 12 and 13), but as the results will show they have a very different bicoherence estimate (Figures 14 and 15).

While the signal of DC bearing fault does not include any QPC components with a bicoherence estimate larger than 0.4, the signal of collector fault includes four QPC components with a $\hat{b}^2 > 0.4$. The difference in the bicoherence of the DC electric-motor faults is significant enough to identify the different types of faults. By using power spectrum estimate these two faults could not be distinguished. The quality of detection of this particular fault by using bispectral analysis is also higher than by using wavelet transform, which was done in one of our recent studies [20].

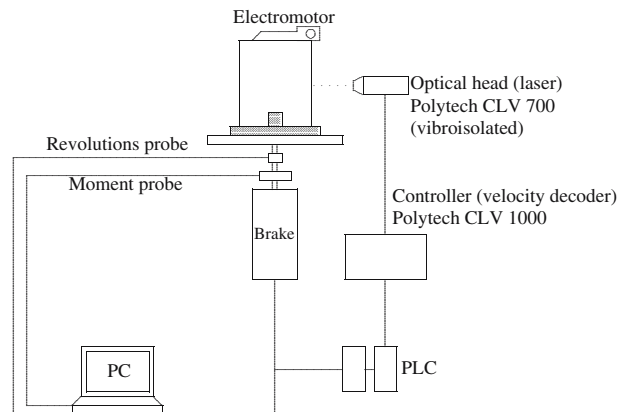


Figure 11. The experimental setup.

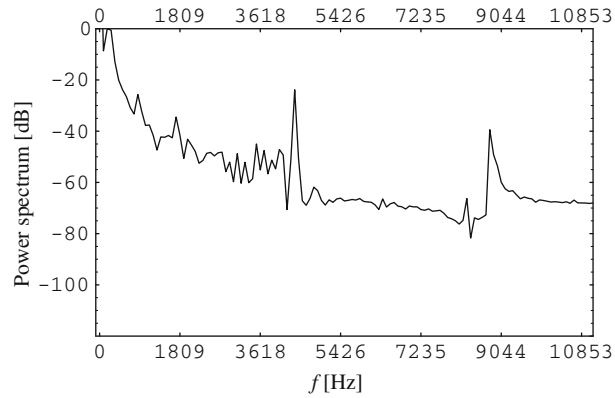


Figure 12. Power spectrum of bearing fault.

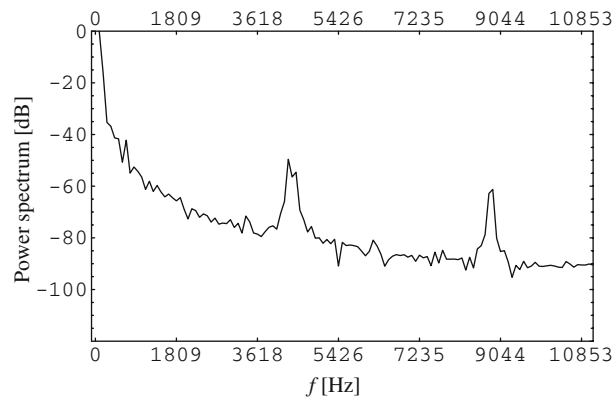


Figure 13. Power spectrum of collector fault.

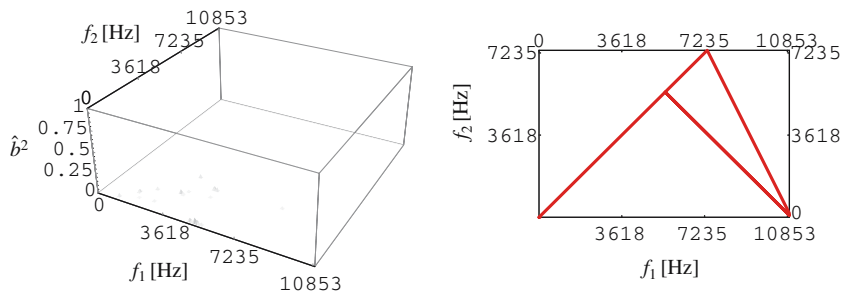


Figure 14. Bicoherence of bearing fault.

7. Conclusions

A short overview of bispectral analysis has been presented. An important advantage of the use of cumulants is that the cumulant of the sum of independent processes is the sum of the cumulants. While the cumulants of harmonic and Gaussian processes are zero the bispectrum cannot detect such processes. This property is used in identification of QPC signals.

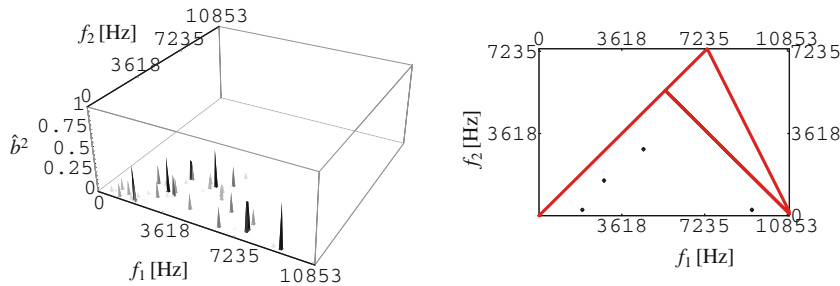


Figure 15. Bicoherence of collector fault.

A numerical example showed that added noise can be used for a better identification of QPC and that a suitable number of segments is required for a successful identification of a process. Using a numerical example it was also shown that up to 5 dB of signal-to-noise ratio the identification of QPC signals is successful, but then rapidly worsens as the noise increases. The numerical experiment showed that the procedures are also blind for harmonic components, even if they are frequency or phase coupled.

While the identification of QPC signals is resistant to noise it is quite sensitive to aliasing. But as Hinich [4] showed, the outer triangle of the bispectrum can be used for identifying the presence of aliasing, and as a consequence, it can be avoided.

Data from a real experiment was used to demonstrate the ability of the bicoherence estimate in condition monitoring to identify different types of manufacturing faults in DC electric motors. As an example, two typical faults with different mechanical causes, but with very similar power spectrum, were analyzed. Their bicoherence estimates differ from each other significantly, and represent a good identification base.

References

1. Boltežar, M. and Hammond, J.K., 'Experimental study of the vibrational behaviour of a coupled non-linear mechanical system', *Mech. Syst. Signal Proce.* **13**(3) (1999) 375–394.
2. Hinich, M.J., 'Testing for gaussianity and linearity of a stationary time series', *J. Time Ser. Anal.* **3**(3) (1982) 169–176.
3. Fackrell, J.W.A., *Bispectral Analysis of Speech Signals*. PhD thesis, The University of Edinburgh, UK, 1996.
4. Hinich, M.J. and Wolinsky, M.A., 'A test for aliasing using bispectral analysis', *J. Am. Statist. Assoc.* **83**(402) (June 1988) 499–502.
5. Zhang, G.C., Ge, M., Tong, H., Xu, Y. and Du, R., 'Bispectral analysis for on-line monitoring of stamping operation', *Eng. Appl. Artif. Intel.* **15**(1) (Februar 2002) 97–104.
6. Yang, D.M., Stronach, A.F. and MacConnell, P., 'The application of advanced signal processing techniques to induction motor bearing condition diagnosis', *Meccanica* **38**(2) (2003) 297–308.
7. Wang, W.J., Wu, Z.T. and Chen, J., 'Fault identification in rotating machinery using the correlation dimension and bispectra', *Nonlinear Dynam.* **25**(4) (August 2001) 383–393.
8. Kocur, D. and Stanko, R., 'Order bispectrum: a new tool for reciprocated machine condition monitoring', *Mech. Syst. Signal Proce.* **16**(2–3) (Mar–May 2002) 391–411.
9. Jeffries, W.Q., Chambers, J.A. and Infield, D.G., 'Experience with bicoherence of electrical power for condition monitoring of wind turbine blades', *IEE proc. Image signal proces* **145**(3) (Jun 1998) 141–148.

10. Simonovski, I., Boltežar, M., Gradišek, J., Govekar, E., Grabec, I. and Kuhelj, A., 'Bispectral analysis of the cutting process', *Mech. Syst. Signal Proce.* **16**(6) (2002) 1111–1122.
11. Boltežar, M., Jakšič, N., Simonovski, I. and Kuhelj, A., 'Dynamical behaviour of the planar non-linear mechanical system – Part II: experiment', *J. Sound Vib.* **226**(5) (October 1999) 941–953.
12. Jakšič, N., Boltežar, M., Simonovski, I. and Kuhelj, A., 'Dynamical behaviour of the planar non-linear mechanical system – Part I: theoretical modelling', *J. Sound Vib.* **226**(5) (October 1999) 923–940.
13. Simonovski, I., Uporaba spektrov tretjega reda pri analizi nelinearnih mehanskih nihanj (Third Order Spectra to the Analysis of Nonlinear Dynamical Systems). Master's thesis, Fakulteta za strojništvo, Univerza v Ljubljani, 1998. In Slovene.
14. Elgar, S. and Sebert, G., 'Statistics of Bicoherence and Biphase', *J. Geophys. Res.* **94**(C8) (August 1989) 10993–10998.
15. Chandran, V. and Elgar, S., 'Mean and variance of estimates of the bispectrum of a harmonic random process – an analysis including leakage effect', *IEEE Trans. Signals Proce.* **39**(12) (December 1991) 2640–2651, citeseer.nj.nec.com/207643.html.
16. Nikias, C.L. and Petropulu, A.P., *Higher-order Spectral Analysis*, Prentice-Hall, Inc., 1993.
17. Simonovski, I., Boltežar, M. and Kuhelj, A., 'Osnove bispektralne analize (Theoretical Background of the Bispectral Analysis)', *Strojniški Vestnik-J. Mech. Eng.* **45**(1) (1999) 12–24.
18. Newland, D.E., *An Introduction To Random Vibrations, Spectral And Wavelet Analysis*, 3rd edn, Addison Wesley Longman Limited, 1993.
19. Haubrich, R.A., 'Earth Noise, 5–500 Milicycles per second', *J. Geophys. Res.* **70**(6) (March 1965) 1415–1427.
20. Boltežar, M., Simonovski, I. and Furlan, M., 'Fault detection in DC electro motors using the continuous wavelet transform', *Meccanica* **38**(2) (2003) 251–264.